Journal of Pharmaceutical Analysis 2014;4(6):351–359

HOSTED BY

Contents lists available at ScienceDirect

Journal of Pharmaceutical Analysis

www.elsevier.com/locate/jpa
www.sciencedirect.com

ORIGINAL ARTICLE

Synthesis of carbon nanosheet from barley and its use as non-enzymatic glucose biosensor

Soma Das, Mitali Saha*

Department of Chemistry, National Institute of Technology, Agartala 799046, Tripura, India

Received 5 November 2013; revised 5 March 2014; accepted 11 March 2014
Available online 29 April 2014

KEYWORDS

Carbon nanosheet;
β-D glucose;
Linear sweep voltammetry;
Square wave voltammetry;
Pharmaceutical analysis

Abstract In this work, carbon nanosheet (CNS) based electrode was designed for electrochemical biosensing of glucose. CNS has been obtained by the pyrolysis of barley at 600–750 °C in a muffle furnace; it was then purified and functionalized. The CNS has been characterized by scanning electron microscopy (SEM), X-ray diffraction (XRD) and Raman spectroscopic techniques. The electrochemical activity of CNS-based electrode was investigated by linear sweep voltammetry (LSV) and square wave voltammetry (SWV), for the oxidation of glucose in 0.001 M H_2SO_4 (pH 6.0). The linear range of the sensor was found to be 10^{-4}–10^{-6} M (1–100 μM) within the response time of 4 s. Interestingly, its sensitivity reached as high as ~26.002±0.01 μA/μM cm^2. Electrochemical experiments revealed that the proposed electrode offered an excellent electrochemical activity towards the oxidation of glucose and could be applied for the construction of non-enzymatic glucose biosensors.

1. Introduction

The continuous development of new nanomaterials for their applications in electroanalytical techniques has been associated with the necessity of the improvement of the quality of efficient electrochemical devices and bio-devices. Nowadays, designing of more sensitive and selective electrochemical devices to recognize the small quantity of analytes has received more and more attention [1]. Carbon-based nanomaterials, especially carbon nanotubes and graphene, are extremely attractive in the bio-analytical area for electrode design as they can combine properties of the high surface area, acceptable biocompatibility, chemical and electrochemical stability and good electrical conductivity [2,3]. Furthermore, many works have shown that the application of different kinds of carbon nanomaterials is receiving more interest in electroanalytical chemistry, because of their effective surface area.

Diabetes has remained a major cause of death and serious vascular and neuropathy diseases. The diagnosis and management of diabetic patients require precise monitoring and control of the glucose level in the body. Therefore, frequent testing of the physiological glucose level is critical in confirming treatment efficiency, preventing long-term complications and avoiding a diabetic emergency, such as hypoglycemic (low blood sugar, <3 mM). This urgency has led to fascinating research and innovative detection strategies in glucose biosensor field. Electrochemical glucose biosensors had their beginning in 1962

*Corresponding author. Tel.: +91 89 7400 6400.
E-mail addresses: mitalichem71@gmail.com, mitalisah@gmail.com (M. Saha).
Peer review under responsibility of Xi'an Jiaotong University.

2095-1779 © 2014 Xi'an Jiaotong University. Production and hosting by Elsevier B.V. Open access under CC BY-NC-ND license.
http://dx.doi.org/10.1016/j.jpha.2014.03.004

reported by Clark and Lyons, who described the measurement of glucose in blood plasma using the enzyme glucose oxidase coupled with a potentiometric electrochemical biosensor. Electrochemical methods based on glucose oxidase (GOx) have played a vital role in simple, easy-to-use blood sugar testing and they have been widely studied over the last few decades for continuous glucose monitoring [4–12].

Enzyme-based sensors show good selectivity and high sensitivity, but their activity is affected by temperature, pH, and toxic chemicals [13,14]. In order to overcome these drawbacks of enzymatic glucose sensors, non-enzymatic glucose sensors have been designed and fabricated, which have several attractive advantages, such as good stability, selectivity and sensitivity and lower detection limit [15–28].

In continuation of our earlier research work of synthesis of carbon nanoparticles from different natural sources [29–32], we have now used barley, which is rich in complex carbohydrates, mainly starch (76%). Interestingly, it gives another nanoform of carbon, i.e., carbon nano-sheet (CNS), after pyrolysis at 600–750 °C in a muffle furnace. A non-enzymatic glucose biosensor was fabricated from CNS and electrochemical studies have been carried out using linear sweep voltammetry (LSV) and square wave voltammetry (SWV). The results showed that the simple preparation procedure coupled with the low cost and high electrochemical activity unfolds a new pathway for economic, reliable and sensitive detection of glucose.

2. Experimental

2.1. Reagents

β-D glucose (99.5%) and H_2SO_4 were purchased from Sigma. All solutions were prepared with deionized water. Pyrolysis of barley was carried out in a muffle furnace (Tanco, PL Tandon & Company, India). The surface morphology of CNS was studied by a scanning electron microscope (FEI Quanta 200 Hv) and X-ray diffraction (XRD) patterns were recorded with JSO ISO DEBYEFLEX 2002 Model X-ray powder diffractometer. Raman spectra were recorded using a Raman spectrometer; WITEC MODEL with 514 nm excitation. Electrochemical studies were performed using a minipotentiostat (Dropsens μstat 100, Spain).

2.2. Synthesis and functionalization of CNS

CNS was synthesized by pyrolysing a cheap and readily available raw material, barley, at 600–750 °C for 2 h under insufficient flow of air in a muffle furnace. The black carbon soot obtained was collected in a thimble and placed into a soxhlet extractor for sequential purification with petroleum ether, acetone, ethyl alcohol and finally with water followed by functionalization with nitric acid. 250 mL of 2 M HNO_3 was stirred with the carbon powder for several minutes and then kept overnight. Excess nitrate was then removed by repeatedly dissolving the black particles in water and then the black particles were evaporated to dryness. The powdered CNS was then characterized by SEM, XRD and Raman spectroscopy.

2.3. Fabrication of CNS electrode

The CNS electrode was fabricated following our reported method [29], just like the commercially available standard electrode DS110 (DRP 110CNT). It was fabricated on an insulating Teflon material containing three silver wires. Both working electrode and counter electrode were made of CNS while reference electrode and electric contacts were made of silver (Fig. 1). Its dimensions is 3.5 cm × 1.0 cm × 0.5 cm (length × width × height) and it is ideal for working with 50 μL volume like the standard electrode.

CNS was first stirred with polystyrene solution, prepared in chloroform (9:1 ratio) followed by sonication. A drop of the slurry was then deposited as a very fine thin film on the Teflon substrate covering two silver wires, serving as working and counter electrodes. The third silver wire was used as a reference electrode.

2.4. Non-enzymatic detection of β-D glucose with fabricated CNS electrode

For non-enzymatic detection of β-D glucose, LSV and SWV studies were carried out at CNS electrode using different concentrations of glucose in 0.001 M H_2SO_4 and maintaining the pH at 6.0. Then, 50 μL of the glucose solution was taken by a micropipette and dropped on the surface of the electrode.

3. Results and discussions

3.1. Characterizations of CNS

SEM images shown in Fig. 2 clearly indicate the formation of carbon nanoparticles arranged in a sheet-like pattern, having width below 50 nm, and Fig. 3 shows the XRD patterns of CNS. Two predominant peaks were observed at around 25.69° and 41.65°, which were assigned for (002) and (111) reflections. Fig. 4 shows the Raman spectra of CNS with two prominent peaks at around 1310 cm^{-1} and 1620 cm^{-1}. The peak having smaller intensity is known as the D band and the peak having greater intensity is known as the G band.

3.2. Mechanism of non-enzymatic glucose detection at CNS electrode

It has been observed that the functionalization of CNS with 2 M HNO_3 leads to the generation of functional groups like hydroxyl (–OH) and carboxyl groups (–COOH) which were suitable for ongoing derivatization reactions [33]. These groups were responsible for the adsorption of glucose molecules on the surface of carbon nanoparticles. The probable reactions are described in Scheme 1 [34]. During the reaction, when β-D glucose reacts with H_2SO_4, it liberates two protons and two electrons, converting into gluconolactone and hydrogen peroxide. On further hydrolysis, the ring structure of gluconolactone breaks into an open structure of gluconic acid.

3.3. Effect of scan rate on the peak current and peak potential of β-D glucose at CNS electrode

LSV was employed to determine the effect of scan rate on the electrochemical detection of β-D glucose at the CNS electrode. Fig. 5 displays 2D and 3D plots of LSV, which show the overlapping of voltagrams of 10^{-5} M β-D glucose (pH ~ 6.0) at various scan rates. The current versus scan rate plot shown in the inset exhibits a linear relationship:

$$Y = -1.3677 + 0.08491X, \quad R^2 = 0.99579,$$

which indicates that the electrochemical kinetics reaction is adsorption-controlled as the adsorption-controlled process should result in a linear plot of current I versus scan rate (ν). The linearity

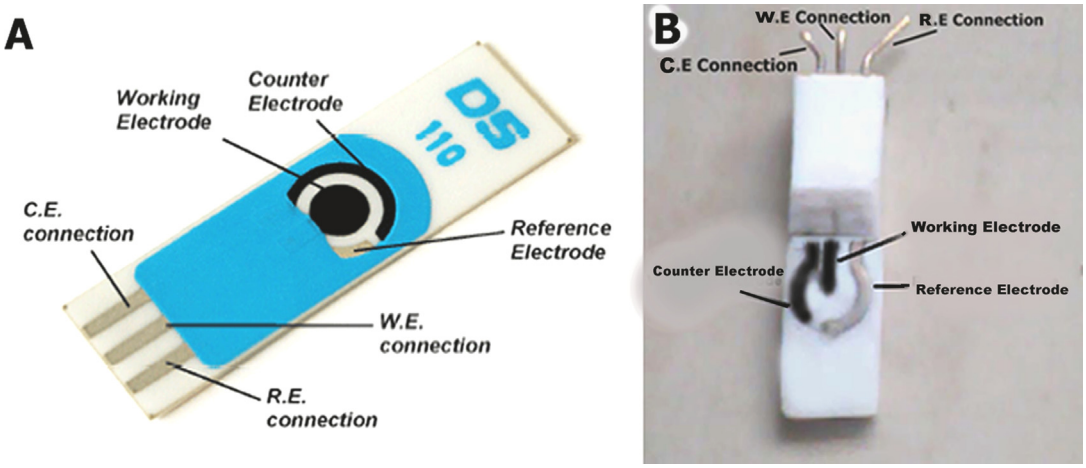

Fig. 1 Images of (A) commercially available standard electrode DS110 (DRP 110CNT) and (B) carbon nanosheet (CNS) modified electrode.

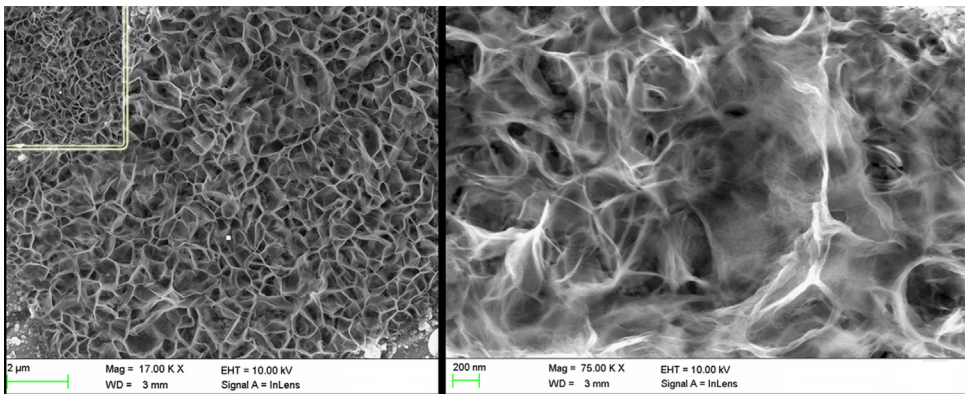

Fig. 2 SEM images of carbon nanosheet (CNS).

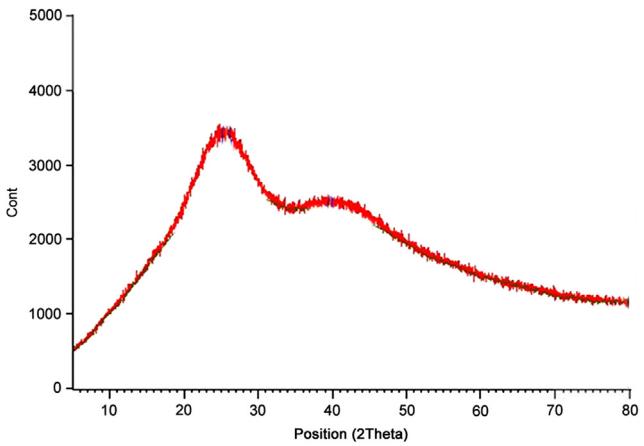

Fig. 3 XRD pattern of carbon nanosheet (CNS).

was observed over the entire range (50–110 mV/s) of scan rates studied with a standard deviation value of 0.20232. In LSV, the potential required for the direct oxidation of β-D glucose at CNS electrodes was found to be −0.08 to −0.09 V. The shifting of potentials may be due to the adsorption of oxidized products of β-D glucose on the electrode surface.

Fig. 6 presents the LSV of 10^{-5} M β-D glucose in 0.001 M H_2SO_4 (pH ~ 6.0) at a scan rate of 100 mV/s at bare silver, glassy carbon and CNS electrodes. Almost no response in peak current was observed at bare silver electrode, indicating that it cannot undergo the reaction in the given potential range. Fig. 6 also shows that though the potential required for the oxidation of β-D glucose at glassy carbon and CNS electrodes was almost equal (~ −0.08 to −0.09 V), the intensity of peak current was found to be much higher in case of CNS electrode.

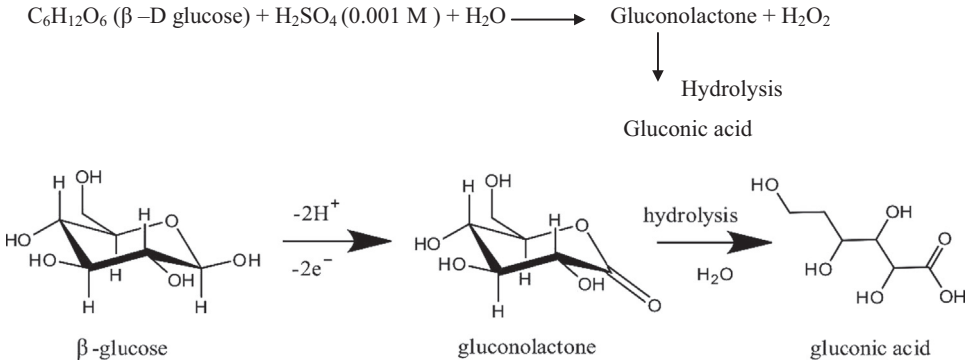

Scheme 1 Oxidation of β-glucose to gluconic acid.

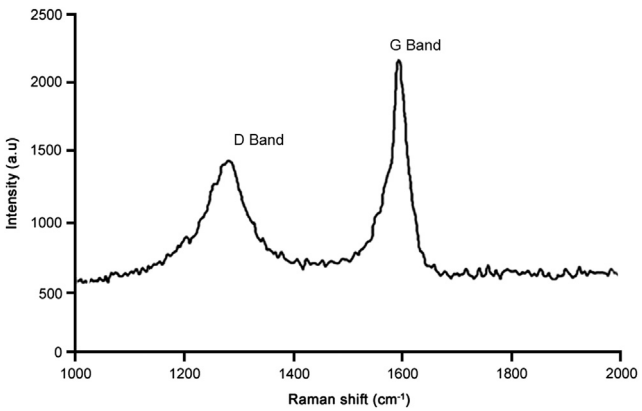

Fig. 4 Raman spectra of carbon nanosheet (CNS).

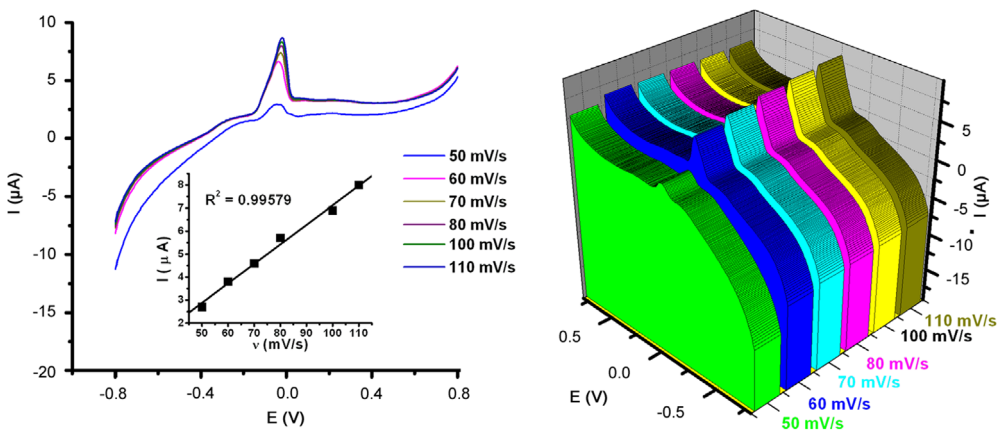

Fig. 5 2D and 3D LSVs of 10^{-5} M β-D glucose in 0.001 M H_2SO_4 at various scan rates (50, 60, 70, 80, 100, and 110 mV/s) on CNS modified electrode at pH 6.0. Inset: The plot of peak current versus scan rate.

3.4. Effect of time interval on the peak current and peak potential of β-D glucose at CNS electrode

Fig. 7 shows the 2D and 3D plots of LSV of 10^{-5} M β-D glucose in 0.001 M H_2SO_4 (pH ~ 6.0) at various time intervals (2–12 min) and at a fixed scan rate of 100 mV/s. Fig. 8 shows the 2D and 3D plots of SWV of the same concentration of glucose in the time interval range of 2–14 min and at 12 Hz frequency (E_{ampl} = 0.010 V). Calibration plots (in inset) showed a linear dependence of the anodic peak current on the entire range of time interval studied in both cases with a correlation coefficient of 0.99849 (Y = 9.76667 + 1.05X) and 0.99535 (Y = 5.67136 + 1.89749X) respectively [35,36]. The standard deviation value was found to be 0.24152 for LSV and 0.91575 for SWV. It may be attributed to the fact that as the time increased, more –OH and –COOH groups were involved in anchoring of the β-D glucose. However, if the study was conducted over an extended time interval range, then a breakdown in the linearity relationship was observed. This may be attributed to the adsorption of oxidized products of β-D

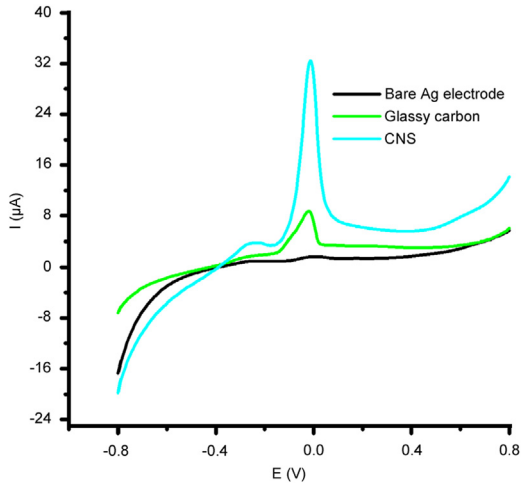

Fig. 6 LSV plots of 10^{-5} M β-D glucose in 0.001 M H_2SO_4 at 100 mV/s scan rate on bare Ag electrode, glassy carbon electrode and CNS modified electrode at pH 6.0.

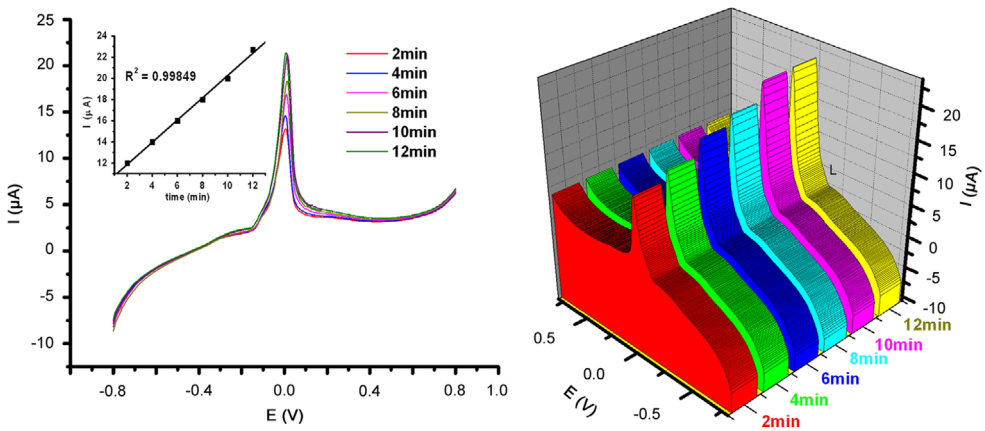

Fig. 7 2D and 3D plots of LSVs of 10^{-5} M β-D glucose at CNS electrode in 0.001 M H_2SO_4 in various time intervals (2, 4, 6, 8, 10 and 12 min) at 100 mV/s scan rate at pH 6.0. Inset: The plot of peak current versus time interval.

glucose on the electrode surface or due to the stabilization of current with time.

3.5. Effect of frequency on the peak current and peak potential of β-D glucose at CNS electrode

Fig. 9 shows the 2D and 3D plots of SWV, which displays the overlapping of voltagrams of 10^{-5} M β-D glucose at the CNS electrode at various frequency rates (7–12 Hz), maintaining the same pH. For SWV studies E_{step} was 0.005 V and E_{ampl} was fixed to 0.010 V. The current versus frequency plot shown in the inset exhibited a linear relationship, confirming the process to be adsorption controlled. The regression equation of $I/\mu A = 3.67619 + 2.15714$ Hz gave an R^2 value of 0.99527. Standard deviation value was found to be 0.44051. The potential required for the direct oxidation of the analyte in the SWV technique was similar to that of the LSV technique (−0.08 to −0.09 V). Therefore, it can be concluded that there was no effect of frequency on the peak potential of the analyte. The intensity of the current was found to increase with the frequency up to 12 Hz, but if the study was conducted beyond 12 Hz, a breakdown in the linearity relationship was observed. This may be due to the adsorption of oxidized products of β-D glucose on the electrode surface.

3.6. Linearity, detection limit, sensitivity and stability of the non-enzymatic β-D glucose sensor

SWV was employed to determine the linearity, detection limit and sensitivity of sensor. Fig. 10(A) shows the plots of SWVs of different concentrations of β-D glucose from 1 to 100 μM in 0.001 M H_2SO_4 at a particular frequency of 12 Hz and E_{ampl} of 0.010 V. It was observed that the oxidation current increased linearly with the increase of β-D glucose in the range of 1–100 μM concentration. The linear regression equation of $I/\mu A = 8.86609 + 2.491$ μM gave an R^2 value of 0.99594. For a better understanding of the lower detection limit, SWV studies with 0–35 μM β-D glucose were done, maintaining the same operating conditions (Fig. 10(B)). The inset showed a linear relationship in the mentioned range of concentration showing an R^2 value of 0.99574. The lower detection limit was found to be 0.802 μM ($S/N = 3$). The sensitivity was calculated using the slope of the current versus concentration calibration plot (Fig. 10 inset) divided by the active

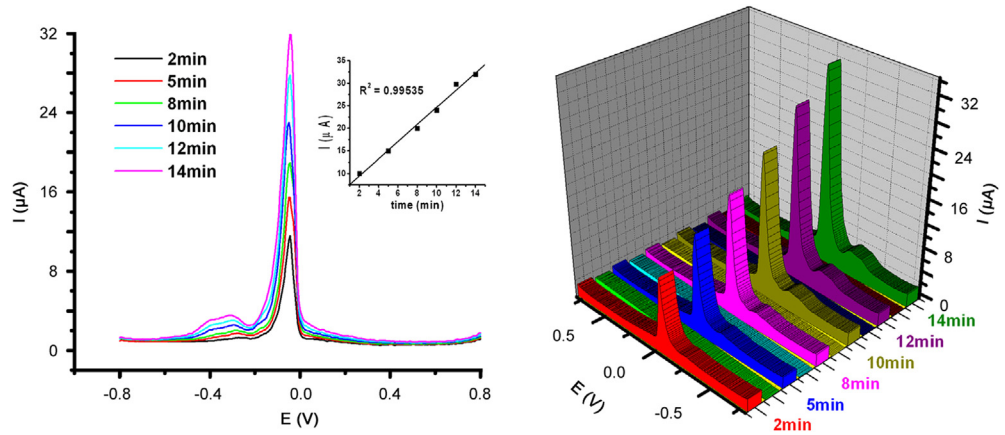

Fig. 8 2D and 3D plots of SWVs of 10^{-5} M β-D glucose at CNS electrode in 0.001 M H_2SO_4 in various time intervals (2, 5, 8, 10, 12 and 14 min) at 12 Hz frequency rate at pH 6.0. E_{step}=0.005 V and E_{ampl}=0.010 V. Inset: The plot of peak current versus time interval.

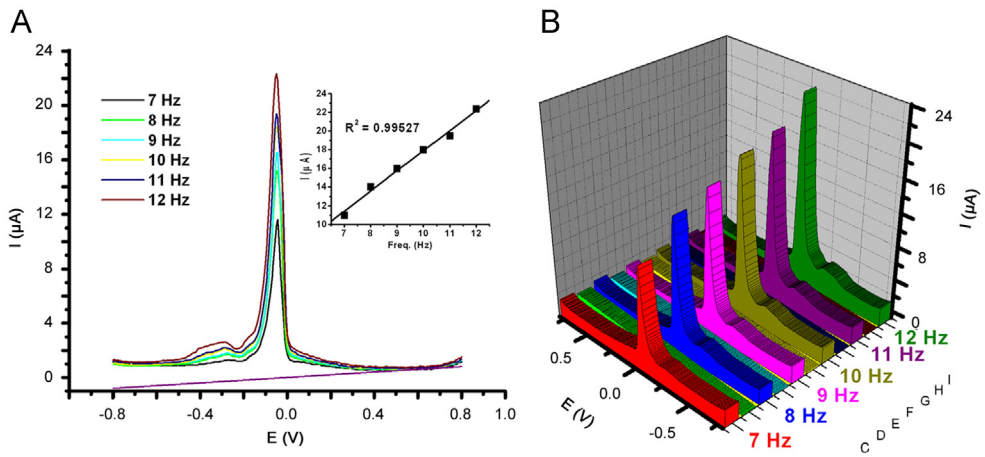

Fig. 9 2D and 3D SWVs of 10^{-5} M β-D glucose in 0.001 M H_2SO_4 at various frequency rates (7, 8, 9, 10, 11 and 12 Hz) on CNS modified electrode at pH 6.0. E_{step}=0.005 V and E_{ampl}=0.010 V. Inset: The plot of peak current versus frequency rate.

Table 1 A comparison of CNS modified electrode with other modified electrodes, using as glucose sensor.

Electrode	Linear range	Detection limit (μM)	Sensitivity	Working potential (V)	Ref.
s-Graphene Ni-NiO	0.1–5 μM	0.28	48270 μA/μM cm^2	0.48	[22]
Pd@Cys-C60/GCE	2.5×10^{-3}–1.0 mM	1	–	−0.05	[26]
Pt19.2/f-CNF80.8/GCE	0–10 mM	0.42	22.7 μA/μM cm^2	–	[27]
Cu/SWNTs/ITO	1.0×10^{-6} -6.0×10^{-4} M	–	1434.67 μA L/mmol cm^2	0.40	[28]
CNS modified electrode	1–100 μM	0.802	~26.002 ± 0.01 μA/μM cm^2	−0.08 to −0.09	**This work**

GCE: glassy carbon electrode; CNF: carbon nanofiber; ITO: indium-doped tin oxide and SWNTs: single walled carbon nanotubes

surface area of CNS according to the following equation [37]:

$$\text{Sensitivity} = \text{slope of the plot}/\text{active surface area of the electrode},$$

where the active surface area of CNS was 0.0958 cm^2 and the slope was 2.491 μA/μM. The sensitivity of the CNS sensor was calculated to be ~26.002 ± 0.01 μA/μM cm^2.

The detection limit, sensitivity and response time of CNS electrode have been compared with those of other reported electrodes used as glucose sensors [22,26–28] (Table 1).

The reproducibility of CNS electrode was determined by SWV (Fig. 11), by fabricating the electrode five times separately, followed by determination of 10^{-5} M glucose. This showed a relative standard deviation (RSD) of 1.43%, demonstrating good reproducibility of the CNS sensor. The stability of the sensor was also explored by storing the electrode in air for 15 days. The current response of 10^{-5} M β-D glucose was found to be stable, keeping ~95% of its initial intensity.

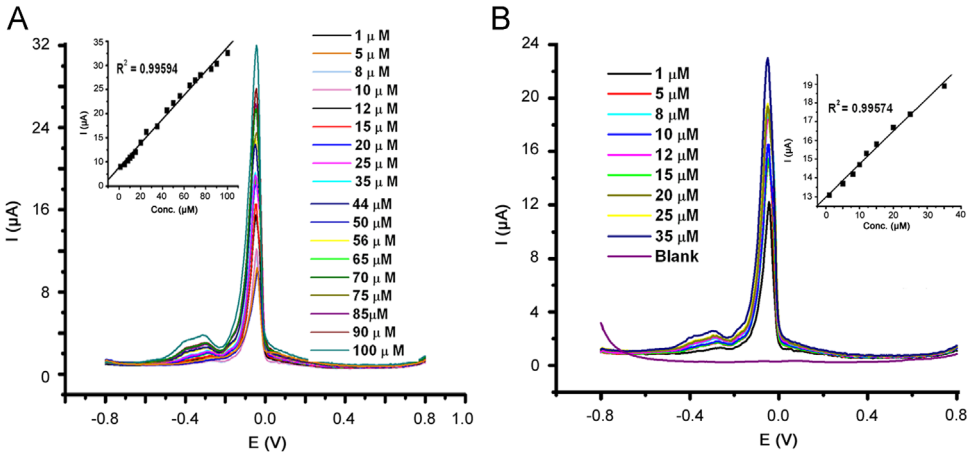

Fig. 10 SWV plots at CNS electrode in 0.001 M H_2SO_4 with (A) 1–100 μM and (B) 0–35 μM of β-D glucose at 12 Hz frequency rate at pH~6.0. E_{step}=0.005 V and E_{ampl}=0.010 V. Inset: Calibration curve of response current versus β-D glucose concentration.

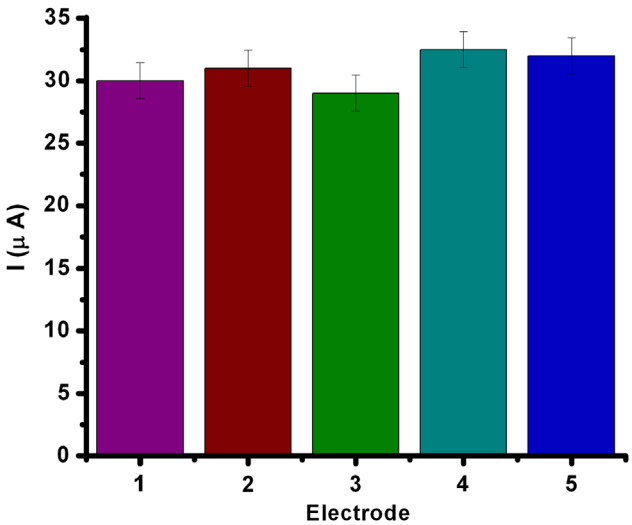

Fig. 11 Stability of the responses for 10^{-5} M β-D glucose obtained at five different modified CNS electrodes. (N=5, RSD=1.43%).

Table 2 Detection results (% Recovery) of glucose in human serum sample.

No. of observations	Glucose added (μM)	Glucose found (μM)	Recovery (%)
1	0.0	1.5	–
2	10.0	11.0	110
3	20.0	22.0	110
4	30.0	31.0	103
5	40.0	42.0	105

3.7. *Interference*

The effects of the presence of some small biomolecules on the current response of 10^{-5} M β-D glucose have been evaluated to describe the selectivity of the reported glucose biosensor. Urea, uric acid, cholesterol, dopamine, fructose, vitamin C, L-alanine, glycine, L-serine, L-phenylalanine, tryptophan and tyrosine have no influence on the current response of CNS electrode at 12 Hz frequency in the potential range from −0.08 to −0.09 V. Since sucrose shows interference at high potential, it did not interfere in the working potential range of −0.08 to −0.09 V. Thus, if the electrochemical studies of biosensors can be performed at a particular potential range, which is low enough and suitable to drive the reaction of interest, then interfering signals can be avoided.

3.8. *Determination of glucose in real samples*

The utility of the proposed method for the non-enzymatic detection of glucose in the real sample was tested by determining glucose in human serum sample at the CNS electrode. The results are summarized in Table 2. The good recoveries of the samples indicate the good applicability of the proposed method for the determination of glucose.

4. Conclusions

In this paper, we have described the detection of β-D glucose by a non-enzymatic way using CNS, obtained by pyrolysing a natural carbon source, barley. The fabricated CNS electrode showed high sensitivity and selectivity, strong stability and good reproducibility towards the sample solution of β-D glucose in the presence of 0.001 M H_2SO_4. Moreover, it exhibited a significant electrocatalytic response towards β-D glucose, within a wide linear range of 10^{-4}–10^{-6} M (1–100 μM) along with a low detection limit of 0.802 μM. The sensitivity and selectivity of the CNS electrode towards the oxidation of glucose proved its effectiveness as a non-enzymatic glucose sensor for practical applications. However, the control of the shape and the size of these carbon nanosheets and their dependency on the mechanism of biosensing are still under investigation.

Acknowledgments

The authors are thankful to AICTE, New Delhi, for the financial support and NEHU, Shillong, for characterizations.

References

[1] A.S.L. Roberto, M.I. Rodrigo, N.C. Frank, Nanomaterials for biosensors and implantable biodevices, in: F.N. Crespilho (Ed.), Nanobioelectrochemistry, Springer-Verlag, Berlin Heidelberghttp://dx.doi.org/10.1007/978-3-642-29250-7_2 (Chapter 2).
[2] P.M. Ajayan, Nanotubes from carbon, Chem. Rev. 99 (1999) 1787–1800.
[3] N. Parviz, F. Farnoush, L. Bagher, et al., Glucose biosensor based on mwcnts-gold nanoparticles in a nafion film on the glassy carbon electrode using flow injection FFT continuous cyclic voltammetry, Int. J. Electrochem. Sci. 5 (2010) 1213–1224.
[4] W. Joseph, Electrochemical glucose biosensors, Chem. Rev. 108 (2008) 814–825.
[5] H.Y. Eun, Y.L. Soo, Glucose biosensors: an overview of use in clinical practice – a review, Sensors 10 (2010) 4558–4576.
[6] A.P. Turner, B. Chen, S.A. Piletsky, In vitro diagnostics in diabetes: meeting the challenge, Clin. Chem. 45 (1999) 1596–1601.
[7] A. Heller, Amperometric biosensors, Curr. Opin. Biotechnol. 7 (1996) 50–54.
[8] A. Heller, B. Feldman, Electrochemical glucose sensors and their applications in diabetes management, Chem. Rev. 108 (2008) 2482–2505.
[9] S.B. Bankar, M.V. Bule, R.S. Singhal, et al., Glucose oxidase: an overview, Biotechnol. Adv. 27 (2009) 489–501.
[10] Y. Zhou, L. Wang, Z. Ye, et al., Mango core inner shell membrane template-directed synthesis of porous ZnO films and their application for enzymatic glucose biosensor, Appl. Surf. Sci. 285 (2013) 344–349.
[11] A.G. Erik, M. Hemanshu, M. Thomas, et al., Reengineered glucose oxidase for amperometric glucose determination in diabetes analytics, Biosens. Bioelectron. 50 (2013) 84–90.
[12] B. Peng, L. Jing, S.B. Anant, et al., Evaluation of enzyme-based tear glucose electrochemical sensors over a wide range of blood glucose concentrations, Biosens. Bioelectron. 49 (2013) 204–209.
[13] Y. Jiao, L. Hyuck, C. Misuk, et al., Nonenzymatic cholesterol sensor based on spontaneous deposition of platinum nanoparticles on layer-by-layer assembled CNT thin film, Sens. Actuators B Chem. 171 (2012) 374–379.
[14] F. Li, J. Song, F. Li, et al., Direct electrochemistry of glucose oxidase and biosensing for glucose based on carbon nanotubes@SnO_2–Au composite, Biosens. Bioelectron. 25 (4) (2009) 883–888.
[15] X. Niu, Y. Li, J. Tang, et al., Electrochemical sensing interfaces with tunable porosity for nonenzymatic glucose detection: a Cu foam case, Biosens. Bioelectron. 51 (2014) 22–28.
[16] E. Shoji, M.S. Freund, Potentiometric sensors based on the inductive effect on the pKa of poly(aniline): a nonenzymatic glucose sensor, J. Am. Chem. Soc. 123 (2001) 3383–3384.
[17] C. Serhiy, C. Chan-Hwa, Gold nanowire array electrode for non-enzymatic voltammetric and amperometric glucose detection, Sens. Actuators B Chem. 142 (2009) 216–223.
[18] J. Wang, D.F. Thomas, A. Chen, Nonenzymatic electrochemical glucose sensor based on nanoporous PtPb networks, Anal. Chem. 80 (2008) 997–1004.
[19] Z. Zhuang, X. Su, H. Yuan, et al., An improved sensitivity nonenzymatic glucose sensor based on a CuO nanowire modified Cu electrode, Analyst 133 (2008) 126–132.
[20] S. Park, H. Boo, T.D. Chung, Electrochemical non-enzymatic glucose sensors, Anal. Chim. Acta 556 (2006) 46–57.
[21] K. Singh, A. Umar, A. Kumar, et al., Non-enzymatic glucose sensor based on well-crystallized ZnO nanoparticles, Sci. Adv. Mater. 4 (2012) 994–1000.
[22] V. Anithakumary, N.T.E. Mary, J. Divya, et al., Nonenzymatic glucose sensor: glassy carbon electrode modified with grapheme-nickel/nickel oxide composite, Int. J. Electrochem. Sci. 8 (2013) 2220–2228.
[23] G. Wang, X. He, L. Wang, et al., Non-enzymatic electrochemical sensing of glucose, Microchim. Acta 180 (2013) 161–186.
[24] S . Liu, B. Yu, T. Zhang, A novel non-enzymatic glucose sensor based on NiO hollow spheres, Electrochim. Acta 102 (2013) 104–107.
[25] F. Huang, Y. Zhong, J. Chen, et al., Non enzymatic glucose sensor based on three different CuO nanomaterials, Anal. Methods 5 (2013) 3050–3055.
[26] X. Zhong, R. Yuan, Y.Q. Chai, In situ spontaneous reduction synthesis of spherical Pd@Cys-C60 nanoparticles and its application in nonenzymatic glucose biosensors, Chem. Commun. 48 (2012) 597–599.
[27] B.J. Singh, E. Dempsey, C. Dickinson, et al., Inside/outside Pt nanoparticles decoration of functionalised carbon nanofibers (Pt19.2/f-CNF80.8) for sensitive non-enzymatic electrochemical glucose detection, Analyst 137 (2012) 1639–1648.
[28] F. Sun, P. Liu, L. Li, et al., Non-enzymatic glucose biosensor based on Cu/SWNTs composite film fabricated by one-step electrodeposition, Chem. Res. Chin. Univ. 27 (2011) 1049–1054.
[29] S. Das, M. Saha, Non enzymatic electrochemical detection of glucose at rice starch-nanoparticles modified electrode, Int. J. Pharm. Bio. Sci. 4 (2013) 967–975.
[30] S. Das, M. Saha, Preparation of carbon nanosphere from bamboo and its use in water purification, Curr. Trends Tech. Sci. 2 (2013) 174–177.
[31] S. Das, M. Saha, Electrochemical studies of carbon nanotube obtained from coconut oil as non enzymatic glucose biosensor, Adv. Sci. Eng. Med. 5 (2013) 645–648.
[32] S.K. Sonkar, M. Saxena, M. Saha, et al., Carbon nanocubes and nanobricks from pyrolysis of rice, J. Nanosci. Nanotechnol. 10 (2010) 1–4.

[33] B. Gebhardt, Z. Syrgiannis, C. Backes, et al., Carbon nanotube sidewall functionalization with carbonyl compounds – modified birch conditions vs the organometallic reduction approach, J. Am. Chem. Soc. 133 (2011) 7985–7995.
[34] E.T. Kathryn, G.C. Richard, Electrochemical non-enzymatic glucose sensors: a perspective and an evaluation, Int. J. Electrochem. Sci. 5 (2010) 1246–1301.
[35] Y. Lin, F. Lu, Y. Tu, et al., Glucose biosensors based on carbon nanotube nanoelectrode ensembles, Nano Lett. 4 (2004) 191–195.
[36] H. Wang, C. Zhou, J. Liang, et al., High sensitivity glucose biosensor based on Pt electrodeposition onto low-density aligned carbon nanotubes, Int. J. Electrochem. Sci. 3 (2008) 1258–1267.
[37] G.N. Dar, A. Umar, S.A. Zaidi, et al., Ce doped ZnO nanorods for the detection of hazardous chemical, Sens. Actuator B Chem. 173 (2012) 72–75.